Intermolecular Association Provides Specific Optical and NMR Signatures for Serotonin at Intravesicular Concentrations

Suman Nag, J. Balaji, P. K. Madhu, and S. Maiti
Department of Chemical Sciences, Tata Institute of Fundamental Research, Colaba, Mumbai 400005, India

ABSTRACT Neurotransmitter vesicles contain biomolecules at extraordinarily high concentrations (hundreds of millimoles/liter). Such concentrations can drive intermolecular associations, which may affect vesicular osmolarity and neuronal signaling. Here we investigate whether aqueous serotonin (a monoamine neurotransmitter) forms oligomers at intravesicular concentrations and whether these oligomers have specific spectroscopic signatures that can potentially be used for monitoring neuronal storage and release. We report that, as serotonin concentration is increased from 60 μM to 600 mM, the normalized fluorescence spectrum of serotonin displays a growing long-wavelength tail, with an isoemissive point at 376 nm. The fluorescence decay is monoexponential with a lifetime of 4 ns at low concentrations but is multiexponential with an average lifetime of 0.41 ns at 600 mM. A 600 mM serotonin solution has 30% less osmolarity than expected for monomeric serotonin, indicating oligomer formation. The proton NMR chemical shifts move upfield by as much as 0.3 ppm at 600 mM compared to those at 10 mM, indicating a stacking of the serotonin indole moieties. However, no intermolecular crosspeak is evident in the two-dimensional NMR rotating frame Overhauser effect spectroscopy spectrum even at 600 mM, suggesting that oligomeric structures are possibly weakly coupled. The appearance of a single peak for each proton suggests that the rate of interconversion between the monomeric and the oligomeric structures is faster than 240 Hz. A stopped-flow kinetic experiment also confirms that the rate of dissociation is faster than 100 ms. We conclude that serotonin forms oligomers at intravesicular concentrations but becomes monomeric quickly on dilution. NMR signatures of the oligomers provide potential contrast agents for monitoring the activity of serotonergic neurons in vivo.

INTRODUCTION

Serotonin is an important neurotransmitter involved in the regulation of mood, sleep, appetite, circadian rhythm, and cognition (1–3). Abnormalities of serotonergic neurotransmission contribute to depression, suicidal behavior, impulsive aggression, eating disorders, obsessive-compulsive disorders, anxiety disorders, alcoholism, and other abnormalities (3–5). Neuronal serotonin is packed to a concentration of hundreds of millimoles/liter in the neurotransmitter vesicles (6,7) and to a level of tens of millimoles/liter in some non-neuronal vesicles (8). Quantum chemical studies indicate that serotonin dimers, trimers, and higher oligomers may be stabilized at high enough concentrations (N. Sathyamurthy, Indian Institute of Technology Kanpur, personal communication, 2007). There is considerable experimental evidence that the indole moiety of serotonin can also participate in stacking interactions (9,10). The stacking of serotonin and ATP molecules is also well documented (11–13). These results suggest that intravesicular serotonin may not exist in a purely monomeric state.

The nature of intravesicular serotonin is interesting for several reasons. An intermolecular association would decrease the effective osmotic pressure of serotonin in the vesicles. The typical osmolality of the cytoplasm is ~290 mOsm (14,15), but the concentration of serotonin itself in the vesicles may exceed this value, as measured by spectroscopic (6) and electrochemical approaches (7,16). In addition, there are considerable amounts of ATP, buffer ions, and other solutes present in the vesicles. An oligomeric association of serotonin, spontaneously forming multimeric structures at higher concentrations, may help the vesicle to balance the osmotic pressure while packing in a large concentration of serotonin.

However, the functional form of serotonin that interacts with the receptors in the postsynaptic cell and with the serotonin transporters is thought to be monomeric, as these exhibit submicromolar-level dissociation constants for serotonin (17). If that is the case, then any oligomer should at most be quasistable and should be able to quickly (within the millisecond timescale of neurotransmission) dissociate when diluted by exocytosis. It is therefore interesting to investigate the nature and stability of intermolecular association of serotonin in aqueous media.

Serotonin concentration quickly drops to submillimolar levels when vesicles are exocytosed during neuronal activity (17,18). However, the overall serotonin concentration in the brain hardly changes, as it is well regulated by the continuing cycle of synthesis, exocytosis, reuptake, and degradation (18). Any experimental parameter that is sensitive to the local dilution of serotonin would present an opportunity to specifically follow the activity of serotonergic neurons. A disruption of intermolecular association is expected to affect the fluorescence spectrum and the lifetime of serotonin and

Submitted September 6, 2007, and accepted for publication December 20, 2007.

Address reprint requests to S. Maiti, Dept. of Chemical Sciences, Tata Institute of Fundamental Research, Homi Bhabha Road, Colaba, Mumbai 400005, India. E-mail: maiti@tifr.res.in.

Editor: Heinrich Roder.

0006-3495/08/05/4145/09 $2.00

doi: 10.1529/biophysj.107.121384

should also change its NMR chemical shift values. The molecular geometry of the interaction can be understood by a rotating frame Overhauser effect spectroscopy (ROESY) type of experiment if the coupling strengths are adequate and if the complex is stable in the timescale of the transfer of magnetization. Fluorescence measurements can in principle have the resolution and sensitivity to follow serotonin release from a single cell (6,8,19), and NMR measurements have the potential to follow such release in a noninvasive manner in vivo. Existing technologies, such as functional magnetic resonance imaging, do not allow the direct monitoring of the activity of specific neuronal subtypes. Positron emission tomography and single photon emission computed tomography imaging allow one to monitor the uptake of radiolabeled serotonin but do not directly measure serotonin exocytosis (20). Capillary electrophoresis can analyze serotonin from extracts of biological tissue, including single cells (21–23), but this method would not be applicable for live cells. Here we explore the optical and NMR spectroscopic properties of serotonin as a function of concentration, with the dual aims of understanding the nature of serotonin at intravesicular concentrations and of identifying spectral signatures associated with serotonin dilution.

MATERIALS AND METHODS

Materials

Serotonin hydrochloride was purchased from Biosynth AG (Staad, Switzerland). Purified water (from a Milli-Q purifier system, Millipore, Billerica, MA) was used throughout to prepare the solutions. To avoid oxidation, nitrogen gas was bubbled through the water before the solutions were prepared. Various concentrations of serotonin hydrochloride salt were prepared, and the pH was determined using pH test strips (Sigma Chemicals, St. Louis, MO).

Methods

Steady-state measurements

The fluorescence spectra at several concentrations were measured in a SPEX Fluoromax 3 spectrometer (Jobin Yvon Horiba, Tokyo, Japan) using a 10 × 2-mm path-length quartz cuvette and using a slit with a nominal band pass of 5 nm. Steady-state fluorescence spectra of several concentrations of serotonin ranging from 60 μM to 600 mM were recorded. All experiments were performed at room temperature. Background intensities were negligible but were subtracted as routine.

Simulation of the fluorescence spectra

The expected fluorescence spectra at high concentration could be simulated from the low-concentration data, assuming no change in the spectral properties. We needed to account for the absorption of the excitation and the reabsorption of the emission by the concentrated solution. The simulations were carried out using the Origin 7.0 software (OriginLab, Northampton, MA). The absorbances for all concentrations c_i were calculated using 1 mM serotonin solution as a standard. The fluorescence spectrum used for this calculation was recorded from a dilute (60 μM) serotonin solution. The area normalized fluorescence spectrum $[N(c,\lambda)]$ with the necessary corrections was simulated using Eq. 1. This treatment follows that of MacDonald et al. (24):

$$N(c,\lambda) = F(c,\lambda)/\int F(c,\lambda)d\lambda, \quad (1)$$

where $F(c,\lambda)$ is given by

$$F(c,\lambda) = F(x,\lambda) \times (1/x) \times (1 - 10^{-A(\lambda,c)})/\varepsilon(\lambda),$$

where $F(x,\lambda)$ is the raw fluorescence of a standard serotonin solution of low concentration (x μM, where $x = 60$ in our case), $A(\lambda, c)$ is the absorption for a given concentration c of serotonin solution (scaled from 1 mM experimental data) for a 2-mm path-length cuvette over all wavelengths λ, and $\varepsilon(\lambda)$ is the molar absorption coefficient at wavelength λ.

Time-resolved measurements

Time-resolved lifetime measurements are carried in a standard 10 × 2-mm path-length cuvette. Details of the apparatus are described elsewhere (25). Briefly, the excitation wavelength is 285 nm, which was obtained by doubling the 575 nm fundamental produced from a Nd:YAG-pumped rhodamine 6G dye laser (Spectra Physics, model No. 375B, Mountain View, CA) operating at 4 MHz. The emission monochromator was set to 420 nm. The excitation polarizer was oriented in the vertical position, whereas the emission polarizer was set to the magic angle (54.7°). A dilute scattering solution (milk powder solution) was prepared to acquire the instrument response function of the entire detection system. All lifetime data are deconvolved with the instrument response function and then fitted using a multiexponential fitting routine. Lifetime data were also analyzed with a maximum entropy method (MEM) fitting routine (26).

NMR measurements

Concentration-dependent one-dimensional (1D) NMR experiments were performed in a Bruker Avance 800 MHz and 500 MHz spectrometer using a presaturation pulse sequence for solvent suppression. All two-dimensional (2D) experiments were done in a Bruker Avance 800 MHz (Bruker/BioSpin, Billerica, MA) spectrometer using the ROESY pulse sequence, with different mixing times (50, 150, 350, and 450 ms). Deuterium oxide (Sigma Aldrich, St. Louis, MO) was used as a locking solvent. All experiments were carried out at room temperature (25°C).

Osmometry

Osmometry was performed using a microvolume osmometer (Model Automatika, Roebling, Berlin, Germany). Osmolality of the different concentrations of serotonin hydrochloride salt solutions ranging from 6 mM to 600 mM was measured. As a control, the osmolality of sodium chloride (S.D. Fine-chem., Mumbai, India) solution was measured over a similar concentration range. The osmolality of water was calibrated to zero in all measurements. All experiments were performed at room temperature (25°C).

Stopped-flow kinetic experiments

Stopped-flow experiments were carried out using a fast stopped-flow fluorescence spectrometer (Bio-Logic, SFM 300, Grenoble, France). Serotonin solution (600 mM) was diluted to 6 mM using nitrogen-bubbled purified water. A 100-fold dilution required the mixing of 1.287 ml of water to 13 μl of serotonin solution. The flow rate was 15 ml/s, yielding a mixing time of ~100 ms. Time-resolved fluorescence counts of serotonin were monitored using an emission filter of 335 nm having a band pass of 70 nm. The excitation monochromator was fixed at 270 nm with the slit set to 5 nm. All experiments were performed at room temperature. Background intensities were negligible but were subtracted from all the data. All data points were recorded with 1-ms time resolution.

RESULTS

Steady-state fluorescence spectroscopy

Emission spectra are recorded as a function of concentration for concentrations ranging from 1 μM to 600 mM, with the excitation fixed at 270 nm. The area-normalized spectra are plotted in Fig. 1. At very low concentrations (between 1 μM and 1 mM), the normalized spectra completely overlap with each other. These data have not been shown separately. At higher concentrations, the long-wavelength tail slowly increases in amplitude. The normalized fluorescence emission spectra show an apparent isoemissive point at ~376 nm. In addition, a small shift in the peak of the emission spectra is also observed as the concentration increases. The peak is at 339 nm for 1 mM serotonin, but it shifts to 345 nm for 600 mM serotonin.

Fluorescence lifetime measurements

An emerging fluorescent species is expected to have a distinct signature in a fluorescence lifetime assay. The fluorescence intensity decay after a near-δ pulse excitation is measured using the time-correlated single-photon counting technique at 420 nm emission wavelength. All lifetime decay data are fitted using a discrete number of components. The decay recorded from a low concentration serotonin solution (62 μM) fits a single exponential (see Fig. 2, *inset*) with a time constant of 4.0 ns (Table 1). This remains similar for all concentrations up to ~2 mM. At concentrations above 5 mM, this value shifts to ~3 ns. The lifetime can be fit by a single exponential up to ~20 mM of serotonin concentration. However, for concentrations >40 mM and up to 75 mM, the data do not fit well to a single exponential but can be fitted with two exponentials. Concentrations above 75 mM require three exponentials (e.g., 600 mM, see Fig. 2, *inset*). Average lifetime decreases monotonically with concentration and becomes ~1.88 ns at 75 mM and as small as ~400 ps at 600 mM (Table 1). To examine whether the finite number of components provides a reasonable interpretation of the data, we also fit our data with a quasicontinuous distribution of lifetimes using a MEM-based analysis routine (26). The MEM analysis (Fig. 2) shows a single peak up to 20 mM, two peaks up to 75 mM, and three peaks above it. The MEM analysis is thus consistent with our interpretation of the lifetime data in terms of a finite number of components.

Osmometry

Osmolality of a solution is the measure of the total number of particles dissolved in the solvent and hence could be used as an indicator for intermolecular association. A 1-molal solution of both serotonin hydrochloride and sodium chloride are expected to have an osmolality of 2 Osm. At concentrations below 150 mM, the osmolality of a serotonin solution behaves as expected (Fig. 3). At higher concentrations, the osmolality starts deviating from linearity. The osmolality is 14% lower for 200 mM and 30% lower for 600 mM compared with the expected value. However, the measured osmolality of 600 mM sodium chloride solution is within 5% of the expected value (Fig. 3). We note that osmolality and osmolarity of the serotonin solutions differ by <10% up to 600 mM of serotonin solution. The solubility of serotonin at 600 mM is checked by centrifuging the solution at 14,000 × *g* for ~2 h. The absorbance of the solution remains unchanged

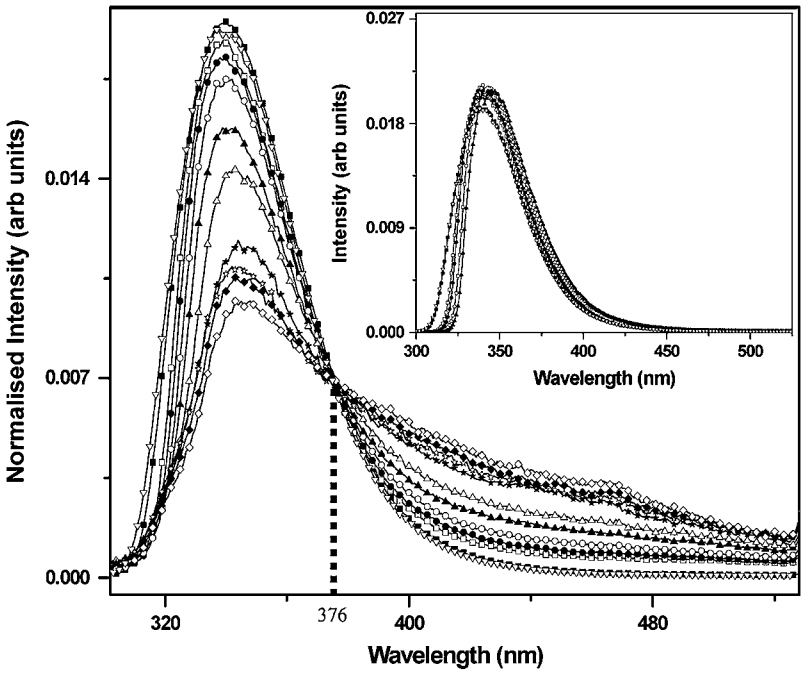

FIGURE 1 Area-normalized fluorescence emission spectra of serotonin at different concentrations: 60 μM (*open inverted triangles*), 1 mM (*solid squares*), 12.5 mM (*open squares*), 25 mM (*solid circles*), 50 mM (*open circles*), 100 mM (*solid triangles*), 200 mM (*open triangles*), 300 mM (*solid stars*), 400 mM (*open stars*), 500 mM (*solid diamonds*), and 600 mM (*open diamonds*). The isoemissive point at 376 nm is shown with the dotted vertical line. (*Inset*) Simulated area-normalized emission spectra of serotonin taking reabsorption of the emission into account; for 60 μM (*open inverted triangles*), 1 mM (*solid squares*), 50 mM (*open squares*), 100 mM (*solid circles*), 300 mM (*open circles*), and 600 mM (*solid triangles*) serotonin. Reabsorption does not appreciably affect the spectra above 360 nm and does not explain the characteristics of the experimentally measured spectra.

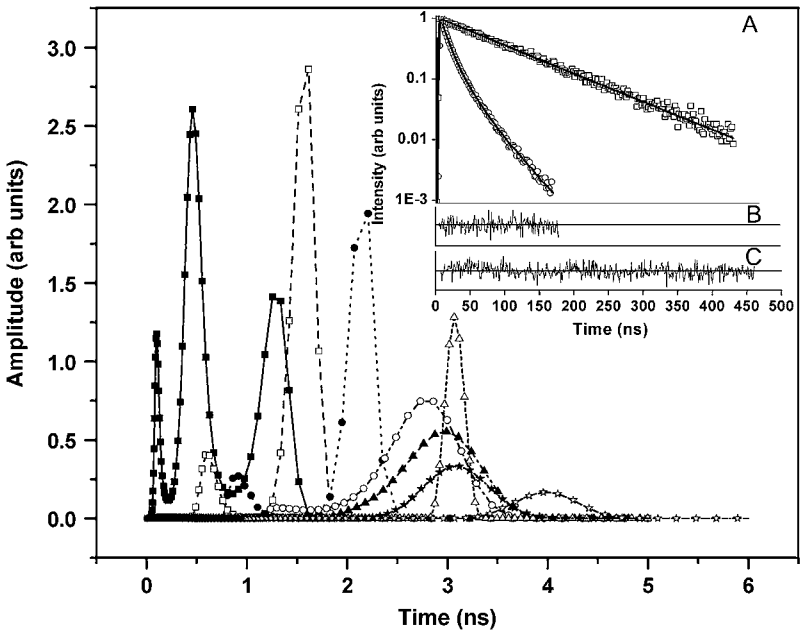

FIGURE 2 Fluorescence lifetime distribution obtained from a MEM-based analysis: 125 μM (*open stars*), 5 mM (*solid stars*), 10 mM (*open triangles*), 20 mM (*solid triangles*), 40 mM (*open circles*), 75 mM (*solid circles*), 150 mM (*open squares*), and 600 mM (*solid squares*). (*Inset, panel A*) Peak normalized fluorescence lifetime decay for 62 μM (*open squares*) and 600 mM (*open circles*) serotonin solution fitted with one exponential and three exponentials, respectively (*solid lines*). (*Inset, panel B*) Residuals for the three-component fit for 600 mM serotonin. (*Inset, panel C*) Residuals for the one-component fit for 62 μM serotonin.

within errors (data not shown). In fact, serotonin remains soluble at least up to 1 M (data not shown).

NMR spectroscopy

Serotonin has seven protons that are stable enough to give clear signatures in an NMR spectrum (Fig. 4, *inset*). Emergence of any new species at higher concentrations should affect the proton NMR spectrum. We record the proton NMR spectrum of serotonin at room temperature as a function of concentration. Fig. 4 shows the spectrum for 10, 25, 50, 100, 150, 200, 300, 400, and 600 mM serotonin. The spectral assignments are indicated on the top, and the numbers correspond to the proton numbers described in the inset. The assignments follow that of Krishnan and Balaram (27). All peak amplitudes are normalized with respect to that of proton 7. The peak appearing ~4.5 ppm is caused by the proton signal from water, which is sometimes not completely suppressed by the saturation pulse. The chemical shifts of all the protons change with concentration, but by different amounts (Fig. 5). The NH proton suffers the largest change of ~0.3 ppm as the concentration goes from 10 mM to 600 mM. The amplitude of this peak (relative to the amplitude of the protons in the alkyl chain) also increases with concentration. Other protons that seem to undergo a significant change of

TABLE 1 Fluorescence lifetime of serotonin as a function of concentrations

Concentration (mM)	τ_1 (ns)	τ_2 (ns)	τ_3 (ns)	α_1	α_2	α_3	τ_{avg} (ns)	χ^2
0.06	4.00	–	–	1	–	–	4.00	0.9
0.125	3.95	–	–	1	–	–	3.95	1.6
0.25	3.96	–	–	1	–	–	3.96	1.3
0.5	3.99	–	–	1	–	–	3.99	1.2
1	3.96	–	–	1	–	–	3.96	1.0
2	4.11	–	–	1	–	–	4.11	1.0
5	3.08	–	–	1	–	–	3.08	1.14
10	3.06	–	–	1	–	–	3.06	1.07
20	2.90	–	–	1	–	–	2.90	1.05
40	2.7	0.77	–	0.91	0.08	–	2.54	1.05
75	2.14	0.54	–	0.84	0.16	–	1.88	1.14
150	1.61	0.84	0.07	0.47	0.15	0.38	0.92	0.97
300	1.46	0.71	0.08	0.26	0.44	0.3	0.71	0.97
600	1.25	0.45	0.07	0.15	0.44	0.41	0.41	0.95

τ_i values are the different lifetime components, α_i values are the corresponding normalized amplitudes, τ_{avg} is the average lifetime, and χ^2 is the reduced chi-square value of the respective fits for different concentrations of serotonin.

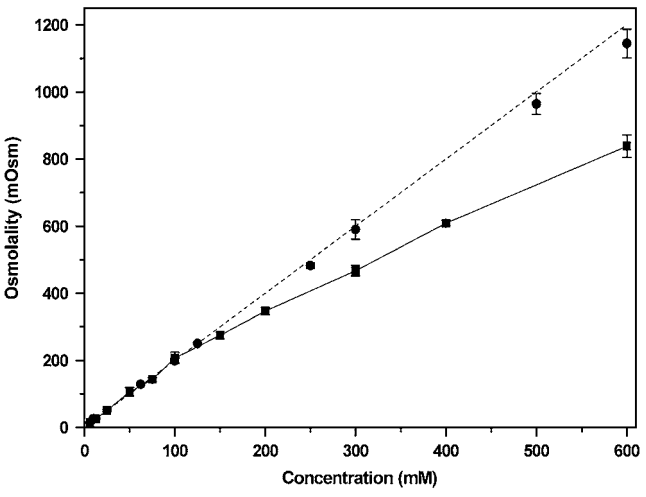

FIGURE 3 Osmolality as a function of serotonin hydrochloride concentration. Serotonin (*solid squares*) and sodium chloride solution (*solid circles*). The dotted line is the theoretical osmolality for any salt of a monovalent cation.

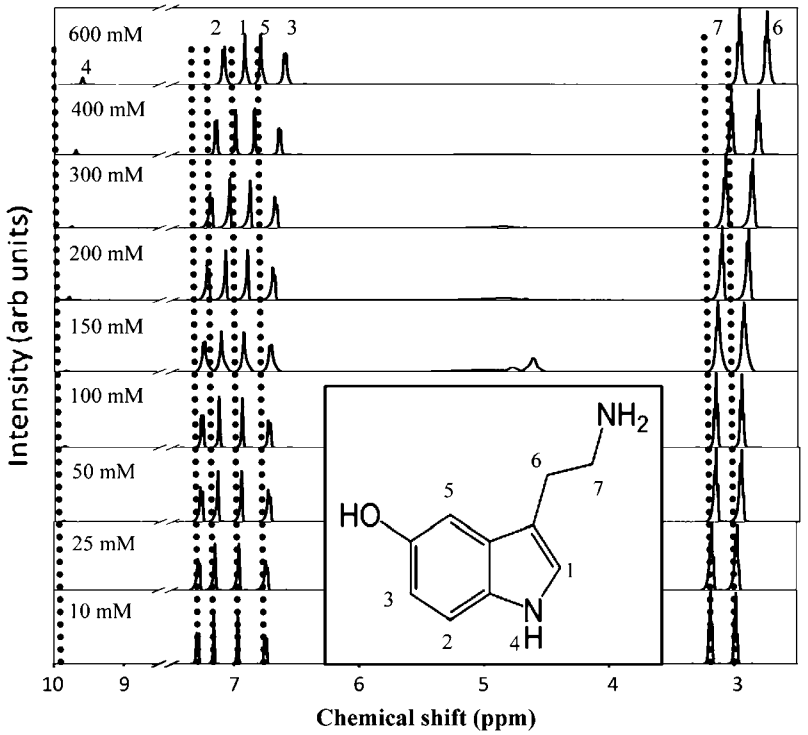

FIGURE 4 Proton NMR spectra of serotonin as a function of concentration. The dotted vertical lines mark the different proton peak positions for 10 mM serotonin. The amplitude of each spectrum is normalized with respect to proton 7. The numbers on top of each peak (for 600 mM) correspond to specific protons of the serotonin molecule (*see inset*). (*Inset*) Chemical structure of the serotonin molecule with different protons marked from 1 to 7.

the chemical shifts (all in the upfield direction) are those of the alkyl chains and the proton attached to the pyrrole ring (Fig. 5). On the other hand, the chemical shifts of the aromatic protons attached to the benzene ring change by comparatively smaller amounts (Fig. 5).

The serotonin solutions are prepared in pure water that does not contain any pH-stabilizing buffer, as it is difficult to buffer such high concentration of solutes. However, we monitor the pH of the solutions. A low concentration of serotonin up to 10 mM has a pH of 7, but the pH becomes somewhat acidic at higher concentrations (it reaches ~5.5 at 600 mM). We investigate whether the difference of pH contributes to the observed change in the chemical shifts and record the proton NMR spectrum of 60 mM serotonin at pH 1 and pH 9. The largest observed change in the chemical shift (in the upfield direction) is ~0.05 ppm (data not shown), which is much less than the difference observed as a result of the change in concentration.

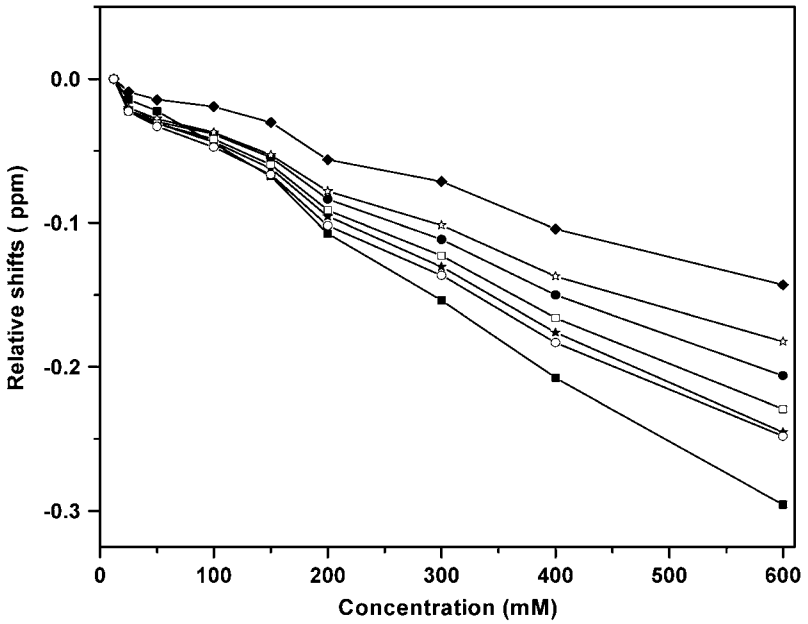

FIGURE 5 Changes in proton chemical shifts as a function of concentration. Proton 1 (*solid stars*), proton 2 (*solid circles*), proton 3 (*solid diamonds*), proton 4 (*solid squares*), proton 5 (*open stars*), proton 6 (*open circles*), and proton 7 (*open squares*); 10 mM serotonin is used as a baseline.

2D NMR spectroscopy

The geometry of any emerging oligomeric species should be manifested in the 2D NMR crosspeaks arising from the intermolecular proton-proton dipolar interactions. We record a high-resolution 2D ROESY spectrum for both a low (6 mM) and a high concentration (600 mM) specimen of serotonin (data not shown). The spectra are recorded at several mixing times (50, 150, 350, and 450 ms). The diagonal peaks in all the spectra are identical to those assigned by the 1D NMR spectrum. All the ROESY crosspeaks observed in the 600 mM spectrum are the same as those observed in the 6 mM spectra and are expected from the monomeric structure of the molecule.

Stopped-flow kinetic experiments

The timescale of the dissociation of the putative oligomers can be directly studied using a stopped-flow apparatus. The 600 mM serotonin is diluted 100-fold (data not shown), and the emission is monitored at 335 nm (excitation is at 270 nm). No appreciable change in fluorescence is observed beyond the mixing time of 100 ms. This experiment puts an upper limit of $\sim$100 ms for the dissociation time of the putative oligomers.

DISCUSSION

Steady-state fluorescence spectra provide evidence for a second species

The existence of an isoemissive point is a clear indication of the coexistence of two different fluorescent species. However, at the concentrations used in this experiment, the inner filter effect (caused by the absorption of the excitation light within the sample cuvette) is considerable. The area-normalization approach, used here, can circumvent the inner filter effect and report the isoemissive point, if one does exist. We note that the spectra would also be affected by the reabsorption of the fluorescence photons by other serotonin molecules. This would change the observed spectra in a wavelength-dependent manner and would shift the peak toward longer wavelengths. We use simulations to investigate whether this can give rise to the spectral features observed here. We measure the absorption spectra for a 1 mM solution and the fluorescence spectrum of a dilute (62 μM) solution, scale them by concentration, and use Eq. 1 to get the simulated area-normalized spectra (Fig. 1, *inset*). We see that this produces relatively small changes above 360 nm, and does not produce an isoemissive point anywhere. We infer that the experimentally observed isoemissive point at 376 nm implies the existence of a new species. The increased amplitude at the longer wavelengths may denote the emergence of dimeric (or higher oligomeric) species, which typically have excited states at an energy that is lower than that of the constituent monomers (28).

We note that the spectral shift of serotonin under different solution conditions is well known. The serotonin emission spectrum is somewhat pH dependent (29). Also, the oxidized form of serotonin develops a long-wavelength shoulder (21,30). However, the concentration-dependent shift observed here differs from these observations. The change is observed even when the serotonin spectra are recorded from a quick dilution of a concentrated solution, suggesting that it cannot be a simple oxidation process. Also, the pH of the solutions varies between 5.5 and 7.0, which is not expected to substantially change the serotonin emission spectrum (29).

Fluorescence lifetime data indicate the emergence of at least two new species

A substantial change in the fluorescence lifetime can indicate the onset of intermolecular interactions. In the simplest case, it can signify the increase of collisional self-quenching in a medium of higher concentration. A plot of the inverse of the lifetime versus the concentration is expected to be linear for a typical Stern-Volmer-type quenching process (28). However, that does not hold true in this case (not shown here, but can easily be seen from the data presented in Table 1). Neither the average nor the longest lifetime components shows an inverse linear variation with concentration. This indicates that the reduction in the average lifetime is not caused by concentration-dependent quenching. Further, at concentrations $>$40 mM, a single exponential component is inadequate to describe the fluorescence decay. Quenching is not expected to lead to extra lifetime components (28). We therefore conclude that collisional quenching, although undoubtedly a contributor at the higher concentrations, cannot explain the observed features of the fluorescence lifetime.

On the other hand, formation of dimers and trimers at higher concentrations is plausible, and these species in general will have different lifetimes. Although the interpretation of any lifetime decay data in terms of a finite number of components may not be definitive, our data are also well supported by the MEM analysis. The MEM analysis fits the data to a quasicontinuous distribution of lifetimes and clearly shows separate peaks emerging at the higher concentrations. Above 150 mM, a third peak appears that signifies the possible existence of a third species. We note that the existence of three species would in general not lead to an isoemissive point in the emission spectrum. However, if the third species has a short lifetime, then its contribution to the steady-state fluorescence intensity may be small. Alternatively, if the spectra of the second and third species are similar, then the isoemissive point may be preserved. In any case, both the steady-state and the time-resolved fluorescence data support the emergence of a new, perhaps oligomeric, species of serotonin at the concentrations prevalent inside neuronal vesicles.

Osmometry provides independent evidence for intermolecular association

Serotonin hydrochloride in water dissociates into protonated serotonin and Cl^-, so for each millimolal of dissolved sero-

tonin, the osmolality of the solution would be 2 mOsm. This is indeed observed for serotonin solutions up to 100 mM (Fig. 3). Sodium chloride used here as a control shows a similar near-linear behavior up to 600 mM (within an error of 5%). However, serotonin clearly deviates from linearity above 100 mM and is 30% below the expected value at 600 mM. Because our solubility experiments show that serotonin remains soluble at least up to 1 M, the osmometry results provide independent evidence that serotonin at high concentrations forms oligomeric structures that coexist with the monomers.

NMR spectroscopy suggests stacking intermediates

1D NMR data show a change in the chemical shift values with concentration. Considerable change occurs at concentrations $\geq$150 mM, which coincides with the appearance of the third peak in the lifetime distribution (Fig. 2) and the deviation from linearity in the osmolality measurements. This correlation of various parameters from different experiments indicates that serotonin starts forming oligomers at concentrations $\geq$150 mM. We rule out a difference of pH (ranging from 7.0 at low concentrations to 5.5 at the highest concentration) as a major contributor to these changes because the chemical shift values change at most by 0.05 ppm (in the upfield direction) as the pH is varied from 1.0 to 9.0. However, spatial proximity of the individual monomers in an oligomer can easily cause such shifts. Intermolecular hydrogen bonding and stacking interactions would be the two most likely mechanisms underlying serotonin oligomer formation. In quantum chemical studies, hydrogen bonding by serotonin has been suggested to cause dimer and trimer formation (N. Satyamurthy, Indian Institute of Technology Kanpur, personal communication, 2007). However, hydrogen bonding would be expected to cause the chemical shifts to be downfield (31), whereas we observe that all the protons shift upfield. The upfield nature of the shifts suggests a stacking interaction of the monomers, which arises as a result of ring current interactions between the two aromatic rings (32). Indeed, many aromatic compounds with similar structures (e.g., nucleic acids and ATP) are known to undergo upfield shifts because of stacking (33–35). In fact, such upfield shifts have been demonstrated by serotonin in interactions with other aromatic molecules (9,12,36). In a pioneering study, Viscio and Prestegard (11) measured the transport of serotonin to the lumens of ATP-rich vesicles by measuring the upfield shift of the serotonin NMR spectrum as it becomes complexed to the ATP. Such ATP-induced upfield shifts have also been observed in the granules of pig platelet cells (13). We therefore suggest that the upfield shifts observed by us are caused by intermolecular stacking interactions between different serotonin monomers.

Possible structure of the serotonin oligomer

The magnitude of the stacking-induced changes in the chemical shifts is expected to be a function of the size of the aromatic rings, their mutual orientation, and the distances between them (37). We observe that protons of the pyrrole ring and those of the alkyl chain undergo larger changes in their chemical shifts compared with those of the benzene ring. This suggests a greater interaction among these moieties in the stacked structure. The indole amide proton also grows in relative strength with concentration (Fig. 5), which suggests that this proton is partially protected by the oligomeric structure formation at the higher concentrations. An alternate possibility is that the relative strength of the amide proton may change as a result of a change in the pH from 7.0 to 5.5 (between the low and the high concentration of serotonin). However, we rule out this possibility because we do not observe any substantial change in the amide signal strength as the pH is varied from 5.5 to 7.0 (at low concentration, data not shown). This is also expected because the pK_a of the indole proton is $\sim$10.0 (29,38,39).

Stopped-flow fluorescence experiments show that the dissociation of the oligomers takes place within the time resolution of the mixing time of the instrument ($\sim$100 ms). This indicates that the oligomers that form at high concentrations are transient in nature and have a stability of $<\sim$100 ms. 1D NMR data show a single peak for each proton at all concentrations. The largest chemical shift change between the highest and the lowest concentrations studied is $\sim$0.3 ppm in an 800-MHz spectrometer. This indicates that the exchange between the two types of structures happens at a rate faster than 240 Hz. The ROESY spectrum also fails to show any intermolecular crosspeaks. Although there could be several reasons for it, including inadequate coupling strength, an explanation that is consistent with our stopped-flow data and the 1D NMR data is the low stability of these complexes. The balance of evidence suggests that serotonin molecules form a new oligomeric entity at high concentrations, most likely by intermolecular stacking, but this entity has relatively low stability (less than a few milliseconds). However, the geometry of such a complex remains to be determined.

The implication of serotonin oligomer formation

Serotonin oligomer formation at intravesicular concentrations has interesting biological and practical consequences. First, the formation of oligomers would aid the ability of the cell to pack very high concentrations of serotonin in submicrometer-sized vesicles against cytosolic osmotic pressure. Our results show that the osmolality of a high-concentration serotonin solution is substantially lower than that expected for monomeric serotonin. We suggest that serotonin oligomer formation plays a significant part in maintaining the extraordinarily high concentrations of serotonin in mammalian neuronal vesicles. We note there are alternative mechanisms that have been proposed to explain the high concentration packing of serotonin into the vesicles. For example, the amperometric ''foot'' signals observed in mast cell exocytosis are thought to be a signature of the slow dissociation of the serotonin mol-

ecules from the proteinaceous matrix (40,41). We also note that there is some evidence that serotonin is associated with a serotonin-binding protein in the vesicular lumen (42). The presence of intracellular ions such as K^+ and Fe^{2+} (43) may also serve as additional means for reducing osmolality. At present it is not clear which, if any, of these is the dominant mechanism.

The second important issue is the effect of such oligomerization on the timescale of serotonergic neuronal communication. If the oligomers were stable, then the receptors and the transporters of serotonin would have to interact with an oligomeric serotonin molecule immediately after exocytosis. However, the receptors and the transporters most likely use monomeric serotonin as a substrate, given their submicromolar binding affinity for serotonin (17). The existence of a stable oligomeric entity would then effectively reduce the number of neurotransmitters in the neuronal vesicle. The ROESY spectrum, the single peaks observed in the 1D NMR data, and the stopped-flow data all indicate that the dissociation of the oligomer happens in less than a few milliseconds. Therefore, the receptors and the transporters may need to interact only with monomeric serotonin during the timescale of the neurotransmission event (about a few milliseconds). Our results therefore suggest that nature has taken advantage of a fast switch between oligomeric and monomeric forms of serotonin to keep the vesicular osmolarity under control on one hand and to keep neurotransmission appropriately fast and efficient on the other.

Finally, the spectral changes associated can potentially allow serotonin-specific investigation of neurotransmission. The serotonin fluorescence from individual vesicles/vesicular clusters in live mammalian neurons can be effectively detected with multiphoton excitation (6,19). In principle, both the fluorescence spectrum and the lifetime can be determined, and serotonin dilution induced by exocytosis can be followed in a quantitative manner. The NMR measurements of dilution are perhaps even more interesting because these can, in principle, be performed in vivo. At present, there is no direct in vivo method to monitor neurotransmitter-specific neurotransmission in the brain. NMR spectroscopy of the brain may be able to record the differential signal associated with the change in the serotonin proton chemical shifts when the serotonergic activity is high. It remains to be tested whether the signal strength is enough to be recorded above the brain background. However, some clinically relevant situations are associated with large serotonin release (such as amphetamine abuse) (44,45), and these may be appropriate candidates for the exploration of this possibility.

We gratefully acknowledge G. Krishnamoorthy, P. K. Nayak, and M. H. Kombrabail for technical support in lifetime and stopped-flow measurements, and we thank N. Periasamy for providing fitting routines for analyzing the lifetime data. We thank N. Naik and the Advanced Centre for Treatment, Research and Education in Cancer, Mumbai, for lending us an osmometer. We are also grateful to the National High Field NMR Facility, TIFR, Mumbai, and M. V. Joshi for all the NMR experiments, and we thank R. V. Hosur and A. Mishra for their help in NMR data analysis. We also thank J. Nowick for valuable scientific insights.

This work was partly supported by a Wellcome Trust Overseas Senior Research Fellowship awarded to S.M. (reference No. 05995/Z/99/Z/HH/KO).

REFERENCES

1. McEntee, W. J., and T. H. Crook. 1991. Serotonin, memory, and the aging brain. *Psychopharmacology (Berl.).* 103:143–149.
2. al-Zahrani, S. S., M. Y. Ho, D. N. Velazquez Martinez, M. Lopez Cabrera, C. M. Bradshaw, and E. Szabadi. 1996. Effect of destruction of the 5-hydroxytryptaminergic pathways on behavioural timing and ''switching'' in a free-operant psychophysical procedure. *Psychopharmacology (Berl.).* 127:346–352.
3. Cooper, J. R., F. E. Bloom, and R. H. Roth. 1996. The Biochemical Basis of Neuropharmacology. Oxford University Press, New York.
4. Coppen, A. J. 1969. Biochemical aspects of depression. *Int. Psychiatry Clin.* 6:53–81.
5. Lapin, I. P., and G. F. Oxenkrug. 1969. Intensification of the central serotoninergic processes as a possible determinant of the thymoleptic effect. *Lancet.* 1:132–136.
6. Balaji, J., R. Desai, S. K. Kaushalya, M. J. Eaton, and S. Maiti. 2005. Quantitative measurement of serotonin synthesis and sequestration in individual live neuronal cells. *J. Neurochem.* 95:1217–1226.
7. Bruns, D., D. Riedel, J. Klingauf, and R. Jahn. 2000. Quantal release of serotonin. *Neuron.* 28:205–220.
8. Maiti, S., J. B. Shear, R. M. Williams, W. R. Zipfel, and W. W. Webb. 1997. Measuring serotonin distribution in live cells with three-photon excitation. *Science.* 275:530–532.
9. Mathur-De Vre, R., and A. J. Bertinchamps. 1974. An NMR study of the relative interaction abilities of different pyrimidine nucleosides with serotonin. *Radiat. Environ. Biophys.* 11:135–143.
10. Helene, C., J. L. Dimicoli, and F. Brun. 1971. Binding of tryptamine and 5-hydroxytryptamine (serotonin) to nucleic acids. Fluorescence and proton magnetic resonance studies. *Biochemistry.* 10:3802–3809.
11. Viscio, D. B., and J. H. Prestegard. 1981. NMR studies of 5-hydroxytryptamine transport through large unilamellar vesicle membranes. *Proc. Natl. Acad. Sci. USA.* 78:1638–1642.
12. Nogrady, T., P. D. Hrdina, and G. M. Ling. 1972. Investigation into the association between serotonin and adenosine triphosphate in vitro by nuclear magnetic resonance and ultraviolet spectroscopy. *Mol. Pharmacol.* 8:565–574.
13. Ugurbil, K., M. H. Fukami, and H. Holmsen. 1984. Proton NMR studies of nucleotide and amine storage in the dense granules of pig platelets. *Biochemistry.* 23:416–428.
14. Bensch, K., G. Gordon, and L. Miller. 1964. The fate of DNA-containing particles phagocytized by mammalian cells. *J. Cell Biol.* 21:105–114.
15. Gordon, G. B., L. R. Miller, and K. G. Bensch. 1963. Fixation of tissue culture cells for ultrastructural cytochemistry. *Exp. Cell Res.* 31:440–443.
16. Bruns, D., and R. Jahn. 1995. Real-time measurement of transmitter release from single synaptic vesicles. *Nature.* 377:62–65.
17. Bunin, M. A., and R. M. Wightman. 1999. Paracrine neurotransmission in the CNS: involvement of 5-HT. *Trends Neurosci.* 22:377–382.
18. Adell, A., P. Celada, M. T. Abellan, and F. Artigas. 2002. Origin and functional role of the extracellular serotonin in the midbrain raphe nuclei. *Brain Res. Brain Res. Rev.* 39:154–180.
19. Kaushalya, S. K., and S. Maiti. 2007. Quantitative imaging of serotonin autofluorescence with multiphoton microscopy. *In* Serotonin Receptors in Neurobiology, A. Chattopadhyay, editor. CRC Press, Boca Raton, FL. 1–18.
20. Laruelle, M., R. M. Baldwin, and R. B. Innis. 1994. SPECT imaging of dopamine and serotonin transporters in nonhuman primate brain. *NIDA Res. Monogr.* 138:131–159.

21. Stuart, J. N., N. G. Hatcher, X. Zhang, R. Gillette, and J. V. Sweedler. 2005. Spurious serotonin dimer formation using electrokinetic injection in capillary electrophoresis from small volume biological samples. *Analyst.* 130:147–151.

22. Benturquia, N., F. Couderc, V. Sauvinet, C. Orset, S. Parrot, C. Bayle, B. Renaud, and L. Denoroy. 2005. Analysis of serotonin in brain microdialysates using capillary electrophoresis and native laser-induced fluorescence detection. *Electrophoresis.* 26:1071–1079.

23. Fuller, R. R., L. L. Moroz, R. Gillette, and J. V. Sweedler. 1998. Single neuron analysis by capillary electrophoresis with fluorescence spectroscopy. *Neuron.* 20:173–181.

24. MacDonald, B. C., S. L. Lvin, and H. Patterson. 1997. Correction of fluorescence inner filter effects and the partitioning of pyrene to dissolved organic carbon. *Anal. Chim. Acta.* 338:155–162.

25. Ramreddy, T., B. J. Rao, and G. Krishnamoorthy. 2007. Site-specific dynamics of strands in ss- and dsDNA as revealed by time-domain fluorescence of 2-aminopurine. *J. Phys. Chem. B.* 111:5757–5766.

26. Swaminathan, R., and Periasamy, N. 1996. Analysis of fluorescence decay by the maximum entropy method: influence of noise and analysis parameters on the width of the distribution of lifetimes. *Proc. Indian Acad. Sci.* (*Chem. Sci.*). 108:39–49.

27. Krishnan, K. S., and P. Balaram. 1976. A nuclear magnetic resonance study of the interaction of serotonin with gangliosides. *FEBS Lett.* 63:313–315.

28. Valeur, B. 2001. Molecular Fluorescence: Principles and Applications. Wiley-VCH, Weinheim, Germany.

29. Chattopadhyay, A., R. Rukmini, and S. Mukherjee. 1996. Photophysics of a neurotransmitter: ionization and spectroscopic properties of serotonin. *Biophys. J.* 71:1952–1960.

30. Zipfel, W. R., R. M. Williams, R. Christie, A. Y. Nikitin, B. T. Hyman, and W. W. Webb. 2003. Live tissue intrinsic emission microscopy using multiphoton-excited native fluorescence and second harmonic generation. *Proc. Natl. Acad. Sci. USA.* 100:7075–7080.

31. Becker, E. D. 1996. Hydrogen bonding. *In* Encyclopedia of Nuclear Magnetic Resonance. D. M. Grant and R. K. Harris, editors. Wiley, New York. 2409.

32. Mitchell, P. R., and H. Sigel. 1978. A proton nuclear-magnetic-resonance study of self-stacking in purine and pyrimidine nucleosides and nucleotides. *Eur. J. Biochem.* 88:149–154.

33. Moon, B. H., V. S. Pai, and E. W. Maynert. 1980. Ring stacking in solutions of norepinephrine and the 4:1 norepinephrine·ATP complex. *Mol. Pharmacol.* 19:44–48.

34. Aradi, F. 1995. Effect of methylation on the pyrimidine-pyrimidine stacking interaction studied by (1)H NMR chemical shift. *Biophys. Chem.* 54:67–73.

35. Lee, D. W., and R. H. Baney. 2004. Oligochitosan derivatives bearing electron-deficient aromatic rings for adsorption of amitriptyline: implications for drug detoxification. *Biomacromolecules.* 5:1310–1315.

36. Schweizer, M. P., A. D. Broom, P. O. P. Ts'o, and D. P. Hollis. 1968. Studies of inter- and intramolecular interaction in mononucleotides by proton magnetic resonance. *J. Am. Chem. Soc.* 90:1042–1055.

37. Hunter, C. A. 1994. Meldola Lecture. The role of aromatic interactions in molecular recognition. *Chem. Soc. Rev.* 23:101–109.

38. Weber, O. A., and V. I. Simeon. 1971. Tryptamine, 5-hydroxytryptamine and 5-hydroxytryptophan complexes of proton and some divalent metal ions. *J. Inorg. Nucl. Chem.* 33:2097–2101.

39. Corona-Avendano, S., M. A. Romero-Romo, A. Rojas-Hernandez, and M. T. Ramirez-Silva. 2005. Study on the stability of the serotonin and on the determination of its acidity constants. *Spectrochim. Acta A Mol. Biomol. Spectrosc.* 61:621–627.

40. Pihel, K., E. R. Travis, R. Borges, and R. M. Wightman. 1996. Exocytotic release from individual granules exhibits similar properties at mast and chromaffin cells. *Biophys. J.* 71:1633–1640.

41. Schroeder, T. J., R. Borges, J. M. Finnegan, K. Pihel, C. Amatore, and R. M. Wightman. 1996. Temporally resolved, independent stages of individual exocytotic secretion events. *Biophys. J.* 70:1061–1068.

42. Tamir, H., K. P. Liu, S. Hsiung, M. Adlersberg, and M. D. Gershon. 1994. Serotonin binding protein: synthesis, secretion, and recycling. *J. Neurochem.* 63:97–107.

43. Tamir, H., and K. P. Liu. 1982. On the nature of the interaction between serotonin and serotonin binding protein: effect of nucleotides, ions, and sulfhydryl reagents. *J. Neurochem.* 38:135–141.

44. Sulzer, D., T. Chen, Y. Lau, H. Kristensen, S. Rayport, and A. Ewing. 1995. Amphetamine redistributes dopamine from synaptic vesicles to the cytosol and promotes reverse transport. *J. Neurosci.* 15:4102–4108.

45. Rudnick, G., and S. C. Wall. 1992. The molecular mechanism of ''ecstasy'' [3,4-methylenedioxy-methamphetamine (MDMA)]: serotonin transporters are targets for MDMA-induced serotonin release. *Proc. Natl. Acad. Sci. USA.* 89:1817–1821.